Electronic Journal of Structural Engineering

Original Article

Cite this: DOI: 10.56748/ejse.23395

Received Date: 09 December 2022
Accepted Date: 30 July 2023

1443-9255
https://ejsei.com/ejse

Assessment of uncertainties in damping reduction factors using ANN for acceleration, velocity and displacement spectra

Abdelhamid Abdelmalek[a,b], Benahmed Baizid[a], Mehmet Palanci[c], Aidaoui Lakhdar[a]
[a] LDMM, University of Djelfa, Algeria.
[b] Civil Engineering Department, University of **Tissemsilt,** Algeria.
[c] Civil Engineering Department, İstanbul Arel University, Istanbul, Turkey

Abstract

Elastic analysis is performed during the design process, and earthquake forces are computed according to standard damped spectral accelerations, which are assumed to be 5% at most. However, buildings are expected to behave nonlinearly instead of linearly due to moderate to destructive earthquakes. Accordingly, the damping factor between the design and actual behaviour of buildings during earthquake excitation differs. This situation increases the uncertainty of the design process for structures exposed to seismic loads and the variation in the reliable estimation of the structures' seismic response. This study is focused on the investigation of the structural damping uncertainties effect on the structure's response spectra through the assessment of uncertainties in the damping reduction factors (DRF) derived from the acceleration, velocity, and displacement spectra. For this purpose, the Monte Carlo method, which relies on repeated random sampling to obtain numerical results, is used for the estimation of the stochastic DRF. The obtained results indicate that the difference between the deterministic and stochastic DRF is around 21% for displacement and velocity and 28.7% for acceleration spectra. Consequently, the DRF derived from the acceleration spectra is more sensitive to the uncertainties inherent in damping than the DRF obtained from displacement and velocity. Therefore, it is important to take this conclusion into account when using these factors. To estimate the calculated DRF values, an artificial neural network (ANN) was developed for the stochastic DRF calculation. The ANN constitutes a simple and efficient method to predict the stochastic DRF since the error obtained is always less than 6%. According to the developed model, practice-oriented results are evaluated for the future evolution of seismic codes.

Keywords

Damping, Uncertainty, Damping reduction factor, Artificial neural network, Response spectra

1. Introduction

Response spectrum analysis is one of the most widespread methods in seismic design and assessment of structures in structural and earthquake engineering. For this purpose, seismic codes typically define the reference spectrum as a 5%-damped pseudo spectral acceleration (PSa) instead of the spectral absolute acceleration (Sa). To encounter other damping values for response spectrum analysis, the damping reduction factor (DRF) is utilized to adjust the reference spectrum.

The DRF is generally estimated from the displacement (Sd) or pseudo acceleration spectra. They have the same values due to their approximate relationship. Several studies were performed to explain the relationship between DRF values derived from displacement (DRFd) or acceleration spectra (DRFa) and their relationship with seismological parameters like magnitude, distance, near and far fault ground motion, pulse like velocity, fault type, ground motion duration, near-source forward directivity and site conditions (Benahmed, 2018; Pennucci et al., 2011; Zhang & Zhao, 2021).

DRFa can be approximated through DRFd and they can be used interchangeably for low structural damping ratios. If the structural damping ratio is relatively large, these quantities can be significantly different especially in high fundamental periods which can be observed in the basic insulation system or structures with additional damping devices. Consequently, using DRFd instead of DRFa may underestimate the inertial forces and present unreliable structural design. In the case of a high damping ratio, using the DRFa instead of the DRFd will lead to a very conservative estimate of the structural seismic responses such as displacement, element forces, etc.

According to (Lin & Chang, 2003), the design force should be the inertial force, and the DRFs should be calculated from the acceleration responses if the damping of structures results from their inelastic response. Otherwise, the design force is the restoring force, and the DRFs should be determined from the displacement responses if the additional energy dissipation devices are dominant in the damping. This is necessary for high-damping systems because smaller DRF resulting from pseudo-acceleration spectra might lead to underestimate of the design seismic forces significantly (Hatzigeorgiou, 2010). The work of (Zhang & Zhao, 2022) showed that the frequency content of the ground movements is one of the main seismological indicators on the PSa and Sa relationship. Otherwise, the damping ratio is the parameter that significantly affects the DRF. (Hu et al., 2022; Liu et al., 2021).

Therefore, errors in the damping estimation can cause inaccurate DRF values and incorrect estimate of structural response. These uncertainties may be a major reason of significant variation in structures and variability of structural responses (Kareem, 1988; Moustafa & Mahadevan, 2011). Hence, it is important to consider these effects while studying the dynamic properties of structures. So far, only a few authors have focused on the impact of damping uncertainty on structural seismic response (Baizid & Cardone, 2021; Benahmed et al., 2017; Benahmed & Hamoutenne, 2018; Haviland, 1976).

The effects of inherent damping uncertainties on DRF were first investigated by Benahmed et al. (Benahmed et al., 2017), where a lognormal probability distribution was used to characterize the damping uncertainty. According to this research, a formulation is proposed to estimate DRF considering 20% of the damping uncertainties (Cvξ). Recent studies (Fiore & Greco, 2020; Greco et al., 2018) investigated the impact of soil type and strong-motion duration on DRF using a stochastic technique with non-stationary input. According to the study of Greco et al., DRF was dependent on the relationship between the spectral period and the dominant period of the ground motion. Greco et al. [2019] provided a method to compute the DRF based on these facts, accounting effective duration, soil type, damping ratio, and natural period.

In this study, attention is focused on the effect of damping uncertainty on DRF estimated from different spectra, displacement, velocity and acceleration. The Monte Carlo approach is employed to produce the random damping values represented by a lognormal distribution. Furthermore, an artificial neural network (ANN) is proposed to estimate the stochastic DRF for different uncertainty levels for DRFd, DRFv and DRFa. The stochastic DRFs are estimated for average plus one standard deviation of the DRF values to prevent the underestimation of DRF values and hence the seismic response of buildings. According to the developed model, practice-oriented results are evaluated for the future evolution of seismic codes.

2. Variability of the dynamic structural response

In structural engineering design, selecting an adequate damping value is a controversial topic. Several researchers worked on its evaluation for various response levels, structural systems, and building typologies. These studies (Haviland, 1976; Kareem & Gurley, 1996) highlighted that the best fitting probability distributions for the damping variation (Cvξ) are the lognormal and the Gamma functions.

The main uncertainty source is the lack of understanding of the damping mechanisms. In addition, the uncertainty inherent in the fundamental period is due to assumptions made in modelling the mass and the stiffness of the structural elements. For instance, some buildings or parts of buildings are used as parking lots, which are function of time (seasons, days), making it highly complicated to estimate the fundamental period in the event of a future earthquake. Furthermore, the soil structure interaction must be considered if the structure is built on soft soil, as the structure's and soil's dynamic characteristics may vary before, during, and after the earthquake. According to previous research (Kareem, 1988), the period uncertainty is represented by a coefficient of variation equal to approximately 0.17.

Haviland (Haviland, 1976) first evaluated the damping coefficient of variation (Cvξ) in the range of 42-87% for the database that consists of real buildings. Kareem then (Kareem, 1988) re-examined the database and observed that the Cvξ ranged between 33 and 78% and suggested that an average value can be taken as 40%. Since the calculated Cvξ values are highly in wide range, these uncertainties should be considered by several methods (Monte Carlo, FORM, SORM, Perturbation method). Amon these methods, Monte Carlo simulation approach (MCS) is the most used tool for quantification of uncertainties, due to its simplicity and robustness. It is a computational algorithm that depends on repeated random sampling to obtain numerical results.

3. Ground motion database of the study

One of the crucial issues in dynamic analysis is the selection of ground motion records that influence the seismic response (Demir et al., 2020; Kayhan et al., 2018). In this study, the database of the Pacific Earthquake Engineering Research (PEER) Center is used since it is easy and accessible for fundamental purposes as a web-based selection tool (PEER, 2016) for practicing engineering in the field.

Firstly, the user defines the response spectrum, and the desired characteristics of the ground motion records such as site classification, magnitude range, shear wave velocity (Vs30), source-to-site distance range, fault type and focal mechanism. Then, the user opts for the seismic records based on the previously defined criteria and provides the best fit to the target response spectrum.

In this study, 62 real ground motion records from different earthquake events are selected. It can be seen from Figure 1 that the moment magnitude, epicentral distance, and Vs30 of selected ground motion range between 4.2 and 7.3, 0 and 100 km, and 200 and 2000 km/s, respectively.

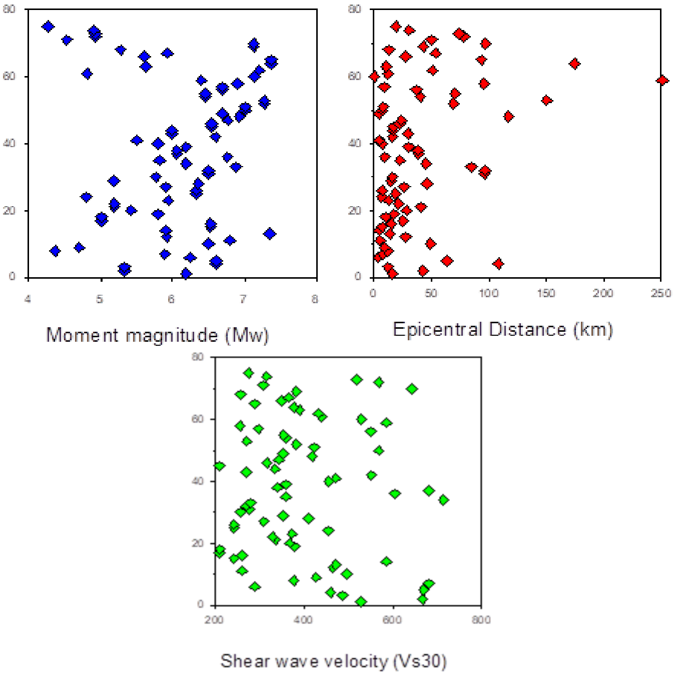

Figure 1. Scatter plot of the selected database.

4. Analysis Results

4.1 Results for deterministic DRF

In this section, a comparison of different deterministic DRF derived from different spectra without considering the damping uncertainties is presented. For this purpose, the response spectra of SDOF systems for each ground motion record were computed considering the damping ratios of 7.5, 10, 20 and 30% for the vibration periods ranging from 0.01 to 4 sec. These spectra were computed in terms of displacements, velocities, and accelerations.

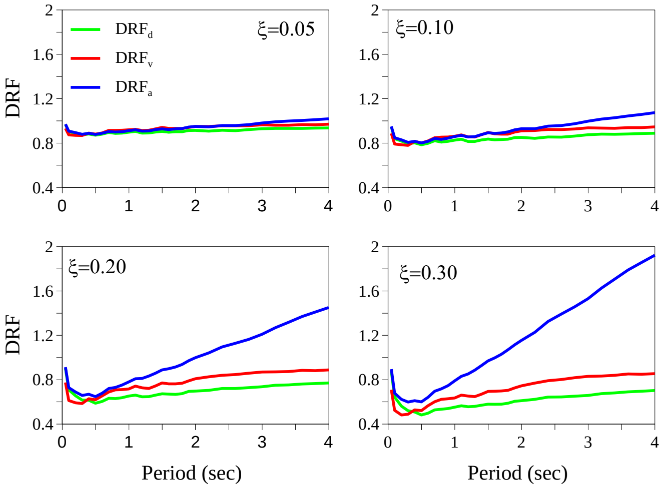

Figure 2. Deterministic DRF obtained through displacement, velocity and acceleration spectra.

Therefore, the average deterministic DRF curves derived from the acceleration DRFa, velocity DRFv and displacement DRFd are estimated and presented in Figure 2 for each damping ratio. These values are deterministic (uncertainty = 0). Results are obtained by the average estimation of the DRF between those of the 62 records.

It can be seen from Fig. 2 that the trend of most DRF values is increasing with increasing vibration periods for all damping ratios considered. However, DRF values obtained from the acceleration spectra present higher values compared to DRF values computed from velocity and displacement.

DRFa values are higher than one for fundamental periods higher than 1.5 sec and reaches 1.9 for =30%. On the other hand, DRFd and DRFv values remain less than one and these values are in the order of 0.8. It is conspicuous that the DRF values higher than one mean that the calculated quantity such as acceleration is higher for higher damping ratios compared to reference damping which is 5% especially for higher structural periods. This situation is valid for DRF values calculated from acceleration spectrum. Similar conclusions are also drawn in the literature about this issue (Lin & Chang, 2003). It should be stated that this situation is natural phenomena since the spectral values in high periods are not sensitive to acceleration.

The results of this analysis conclusively show that using one of these DRFs without first determining which one is best to evaluate high damping response spectra can only be effective at low levels of damping. The use of the wrong one can seriously affect the structure's reliability, mainly for high values of damping and fundamental periods.

4.2 Results for stochastic DRF

Due to the significant value of the damping uncertainties (mainly ranging between 33 and 78%), it is important to take this uncertainty into account when designing structures. As previously considered, the damping ratio is a random variable that follows the log-normal distribution. Therefore, the Monte Carlo method can be used to take this uncertainty into account. In this study, 200 values of damping for each period value were computed by using the Monte Carlo method for each spectrum type such as acceleration, velocity and displacement. Accordingly, 200 DRF values were estimated. The distribution of the DRF resulted is not lognormal because the relation between ξ and DRF is not linear.

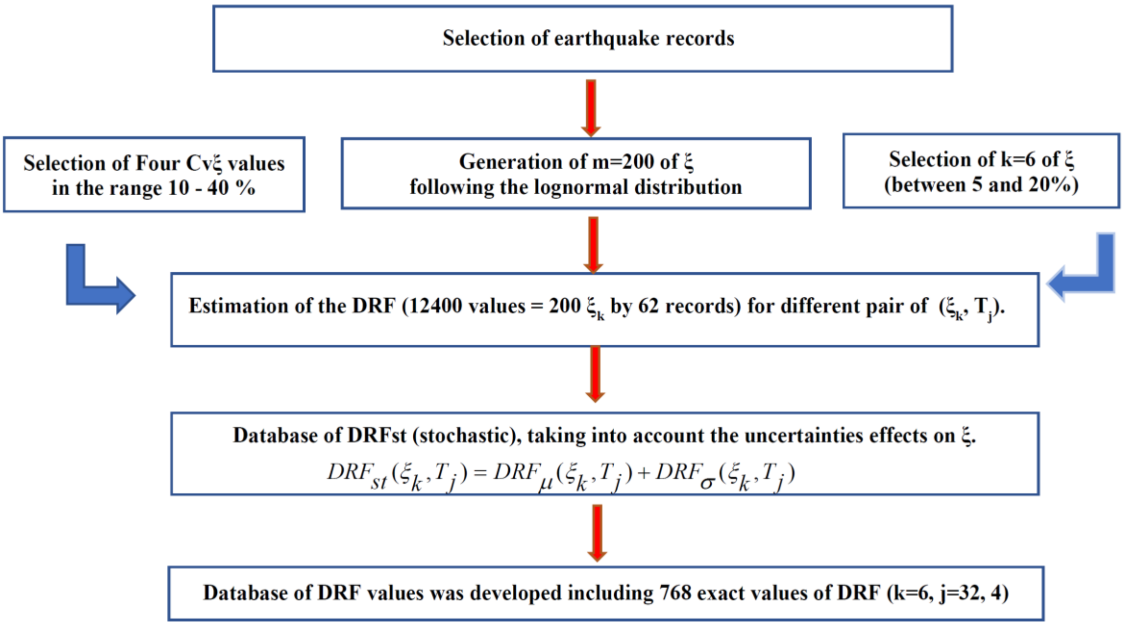

Figure 3. Multistep procedure flowchart

Following the determination of DRF values, the mean (DRFμ) and standard deviation (DRFσ) of DRF values were computed for displacement, velocity and acceleration spectra associated to each period of vibration. Later, the stochastic value of DRFst depending on the damping and the period is computed using the DRFμ and DRFσ values via Eq. 1. According to this equation, the stochastic DRF is the sum of average DRF and one standard deviation of the DRF.

$$DRF_{st}(\xi_k, T_j) = DRF_{\mu}(\xi_k, T_j) + DRF_{\sigma}(\xi_k, T_j) \qquad (1)$$

Figure 3 is used to describe a flowchart of multistep procedure for the developed database used in this paper. In Fig. 4, three curves describing the deterministic DRF and stochastic DRF for =10 and 40%, are drawn. The computed values correspond to the average spectra of the 62 individual spectra associated to the damping values generated by Monte Carlo method. These curves are given for displacement, velocity and acceleration spectra.

It should be noted that regardless of the value taken into consideration, the DRFd and DRFv curves exhibit almost the same trend. Evidently, as the value rises, the difference between the stochastic and deterministic curves is increasing.

The difference between the deterministic and the stochastic DRF is presented in Table 1. For =10%, the differences between the deterministic and the stochastic DRF values for DRFd, DRFv and DRFa is almost the same for =5%. This differences slightly increases for DRFa for ξ=20 % and equal to 4.8 ,4.5 and 7.0% respectively.

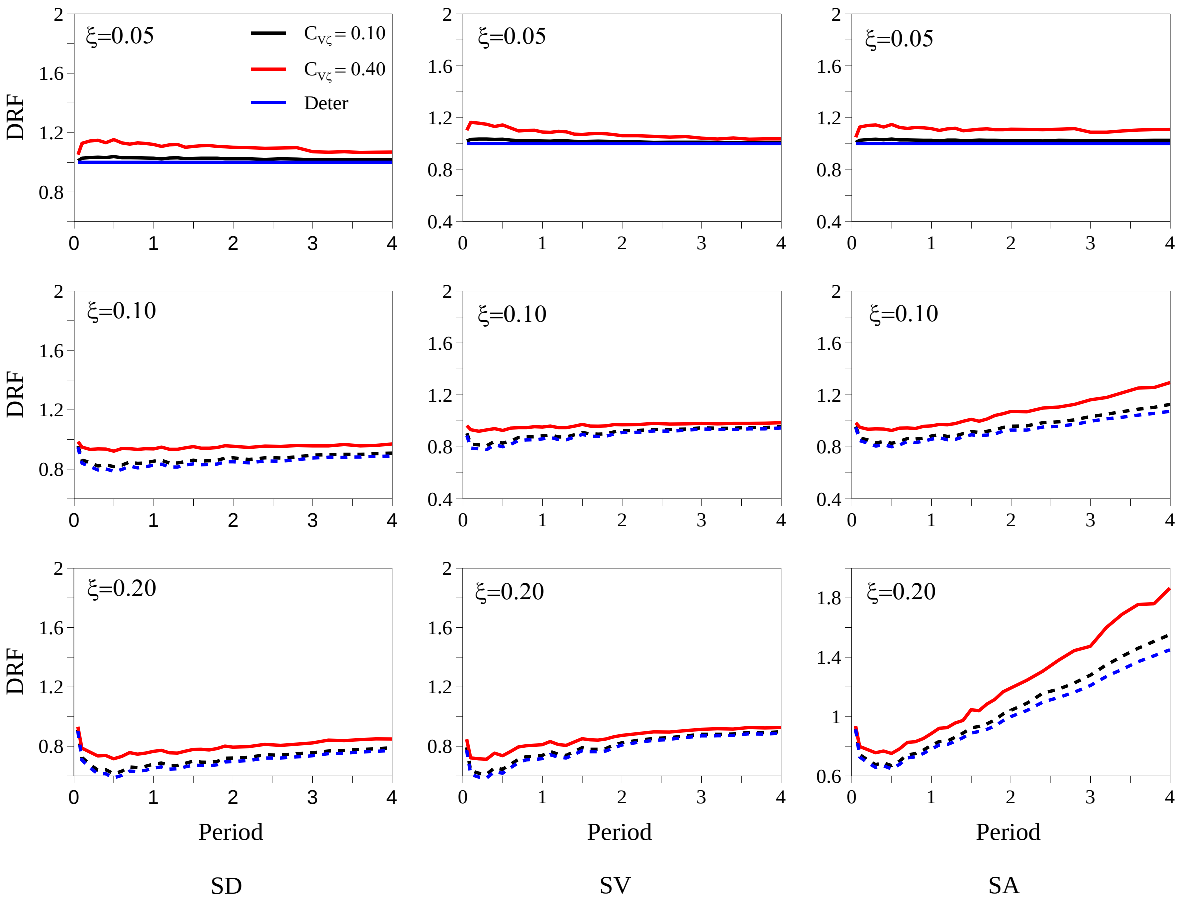

Figure 4. Stochastic DRFd , DRFv and DRFa

Table.1. Error between the deterministic and the stochastic DRF

		ξ=5	ξ=10	ξ=20
$C_{v\xi}$ = 10	DRF_d	3.7%	4.0%	4.8%
	DRF_v	3.6%	3.9%	4.5%
	DRF_a	3.6%	5.0%	7.0%
$C_{v\xi}$ = 40	DRF_d	15.3%	17.9%	21.9%
	DRF_v	16.3%	19.3%	21.8%
	DRF_a	14.8%	20.6%	28.7%

Similar results are obtained for = 40%, where the difference is around 21% for DRFd and DRFv and 28.7 % for DRFa. Consequently, the DRF derived from the acceleration spectra is more sensitive to the uncertainties inherent in damping than the DRF obtained from displacement and velocity. It appears that the DRF values are higher than the comparable deterministic values when the uncertainties are considered. In other words, lower spectral ordinates, or lower design base shear or design displacement, can be estimated if the uncertainties in damping are not taken into account, which means an over conservative design.

To better understand the uncertain DRF curve variability for different cases, the stochastic DRF curves were normalized by the deterministic ones and presented in Figure 5 for DRFd, DRFv, DRFa.

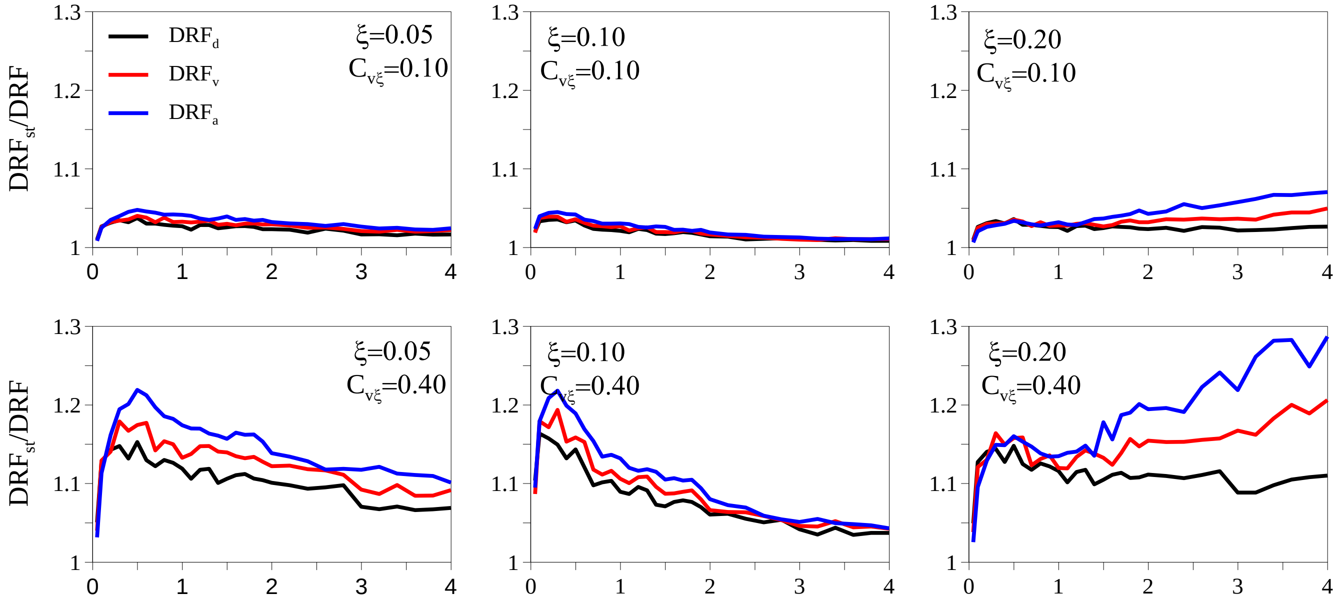

Figure 5. Stochastic /determinist values for DRFd, DRFv, DRFa

For lower damping ratios, the trend of ratios is very close and similar. On the other hand, DRFst/DRF derived from acceleration has higher values than those derived from velocity and displacement. This confirms that DRFs derived from acceleration responses are more sensitive to damping uncertainty than DRFs derived from displacement responses. It is important to take this conclusion into account when using these factors.

5. Artificial Neural Networks

5.1 Network design

Neural networks constitute a branch of artificial intelligence that has recently undergone rapid evolution and progress. It has the capability of learning the patterns for the definition of the relationship between the input and output of a certain test or process that can later be used to predict new conditions for which the results (output) are not known. Neural networks have been developed from a simple architecture to various types of complex structures, such as convolutional neural network (CNN) and recurrent neural network (RNN) (Challagulla et al., 2022; Hiew et al., 2023). In this study, the ANN model was constructed using one of the most widely used types of ANN, which is the feed-forward multi-layer neural network (MLF).

A MLF neural network consists of neurons that are ordered into layers (Fig. 6). The first layer is called the input layer, the last layer is called the output layer in which the neurons are distributed in layers in such a way that two consecutive layers are fully connected; all the neurons of an input layer receive the outputs of all neurons in the previous layer.

In feed-forward ANN, the neurons are organized in layers. There are no connections among neurons within the same layer and connections only exist between successive layers. Each neuron from layer l has connections to each neuron in layer l + 1. A signal propagates from the input layer to the output layer through several hidden layers.

For each set of input signals, feed forward ANNs allow information to travel one way only; from input to output. There is no feedback (loops) i.e., the output of any layer does not affect that same layer. A cell performs a weighted sum in which a transfer function is applied, and the output is transmitted to the following layer. The transfer function allowing to calculate the cell output is often a linear sigmoidal function. The number of hidden layers, the number of cells per layer and their connections define the architecture of the neural network.

Neurons in each layer are connected together by a weight coefficient. There is a transfer function that changes inputs into output. It is necessary to train ANN before application and neural training is a method used to calculate the synaptic weights and bias in an iterative way until produces data compatible outputs. During training, the network works with iterative method until it produces a new output. At the beginning of the training process, initial weights are randomly given to the connections. Inputs are inserted into the input layer and then move forward through the hidden layer of neurons to the output layer. At the end, outputs would be compared with real outputs (Benahmed & Hamoutenne, 2018).

The choice of network architecture has a significant impact on model precision and computational time. Therefore, several techniques to determine the number of hidden nodes in a hidden layer are discussed in literature (Sheela and Deepa, 2012). One of these methods is to train and evaluate the ANN using a small number of hidden layers neurons. The number of hidden neurons was then increased. Repeat the approach above until the user's training and testing have improved and the error has become acceptable in successive iterations. In this study, the optimal number selected is taken equal to 40. The ANN architecture obtained is presented below as 3-60-1 (see Fig. 6).

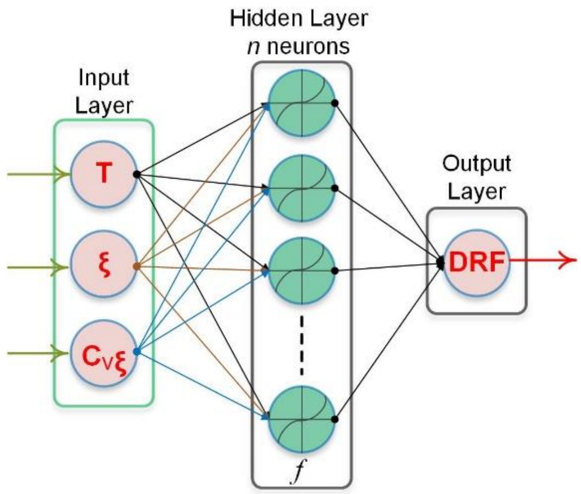

Figure 6. Feed-forward multi-layer neural network.

5.2 Correlation analysis

For the efficiency appreciation of the selected network, the whole data (used for learning, validation and testing) was passed over the network to perform a regression among the network output values and the corresponding target values.

A comparison of both values is given in Fig. 7. It can be seen from the figure that the fitting lines are almost diagonal, and the correlation coefficient (R) is almost equal to one. Therefore, it can be claimed that the ANN output values are in very good agreement with those computed in the database. The computed regression coefficients are R= 99.82%, 99.80%, 99.78% for DRFd, DRFv, and DRFa , respectively.

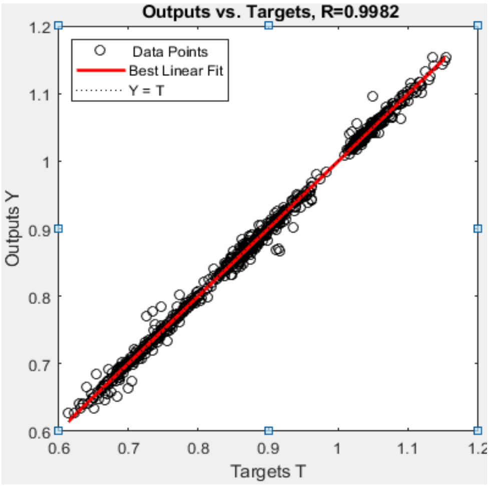

DRFd

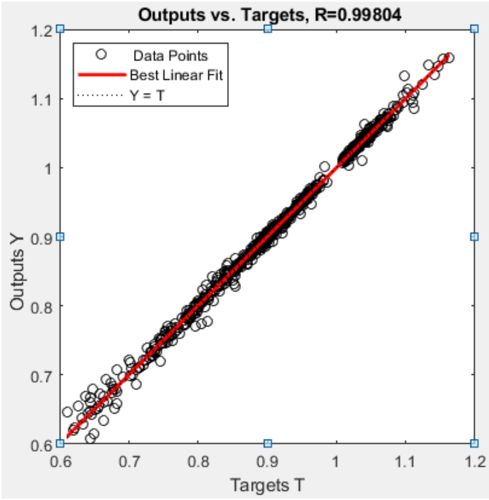

DRFv

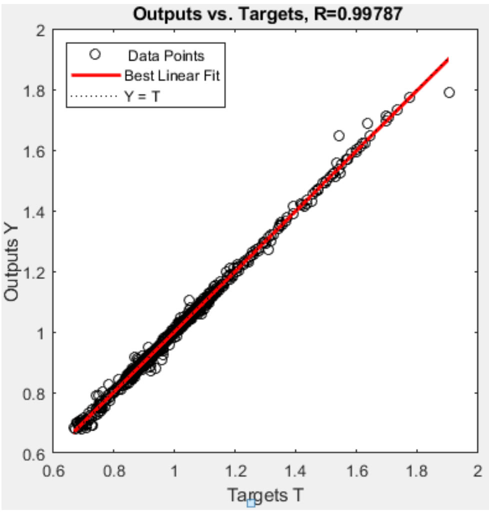

DRFa

Figure 7. Neural network outputs against target DRF values.

5.3 Relative error

The efficiency of the proposed method ANN is verified through the computation of relative error between stochastic DRFst estimated by the Eq.1 and the DRFst estimated by the ANN using Eq.2.

$$Err = \left| \frac{DRF_{real} - DRF_{ANN}}{DRF_{real}} \right| \quad (2)$$

Calculations have revealed that the obtained relative errors committed by ANN is always less than 6%. The maximum value of this relative error was computed as 5.8% for DRFd, 4.8% for DRFv and 6.6% for DRFa. The average relative error was computed as 0.59% for DRFd, 0.56% for DRFv and 0.72% for DRFa if relative errors for all DRFs are used in the database. The ANN constitutes a sample-based, effective approach for predicting the stochastic DRF values. Accordingly, it can be stated that DRF values obtained from the ANN almost perfectly match with real DRF outcomes.

6. Concluding Remarks

The influence of the damping uncertainties on the DRF obtained from the displacement, velocity, and acceleration responses has been investigated in this study. Also, a method for determining the stochastic DRF based on the ANN was proposed. The suggested method clearly accounts for the uncertainties associated with structural damping. Based on the results, some conclusions and suggestions can be summarized as follows:

It is conspicuous that the difference between the DRFa and DRFd and DRFv becomes more significant for higher values of damping and fundamental periods.

Evaluation has shown that DRFst values have the same tendency for low damping (=5%) ratios. On the other hand, the difference between the deterministic and the stochastic DRFs becomes significant mainly for T > 1.5 sec and higher damping ratios. Similar results are obtained for = 40% where the error is around 21% for DRFd and DRFv and 28.7% for DRFa.

It is apparent from the results that DRF values are higher than deterministic values when the uncertainties associated with structural damping are accounted for. This situation implies that the use of deterministic DRF values might underestimate the design base shear or displacements if the uncertainties in damping are not taken into account especially at lower spectral ordinates.

It is observed that the relative error between the real and predicted DRF values from ANN is very low, always less than 6%. It is evident from these results that estimations of ANN have very good agreement with real computed DRFs.

References

Baizid, B., & Cardone, D. (2021). ESTIMATION OF STOCHASTIC DAMPING REDUCTION FACTOR USING MONTE CARLO SIMULATION AND ARTIFICIAL NEURAL. Ingegneria Sismica, International Journal of Earthquake Engineering, 04, 37–52.

Benahmed, B. (2018). Formulation of damping reduction factor for the Algerian seismic code. Asian Journal of Civil Engineering, 19(4). https://doi.org/10.1007/s42107-018-0023-6

Benahmed, B., Hammoutene, M., & Cardone, D. (2017). Effects of damping uncertainties on damping reduction factors. Periodica Polytechnica Civil Engineering, 61(2), 341–350. https://doi.org/10.3311/PPci.9665

Benahmed, B., & Hamoutenne, M. (2018). Use of the Artificial Neural Networks to Estimate the DRF for Eurocode 8. Periodica Polytechnica Civil Engineering, 62(2), 470–479. https://doi.org/10.3311/PPci.8139

Challagulla, S. P., Bhargav, N. C., & Parimi, C. (2022). Evaluation of damping modification factors for floor response spectra via machine learning model. Structures, 39, 679–690. https://doi.org/10.1016/J.ISTRUC.2022.03.071

Demir, A., Palanci, M., & Kayhan, A. H. (2020). Evaluation of Supplementary Constraints on Dispersion of EDPs Using Real Ground Motion Record Sets. Arabian Journal for Science and Engineering, 45(10), 8379–8401. https://doi.org/10.1007/S13369-020-04719-9/METRICS

Fiore, A., & Greco, R. (2020). Influence of Structural Damping Uncertainty on Damping Reduction Factor. Journal of Earthquake Engineering, 00(00), 1–22. https://doi.org/10.1080/13632469.2020.1747573

Greco, R., Fiore, A., & Briseghella, B. (2018). Influence of soil type on damping reduction factor: A stochastic analysis based on peak theory. Soil Dynamics and Earthquake Engineering, 104(October 2017), 365–368. https://doi.org/10.1016/j.soildyn.2017.10.020

Hatzigeorgiou, G. D. (2010). Damping modification factors for SDOF systems subjected to near-fault , far-fault and artificial earthquakes. March, 1239–1258. https://doi.org/10.1002/eqe

Haviland, R. W. (1976). A study of the uncertainties in the fundamental translational periods and damping values for real buildings. Res. Rep. No. 5, Pub. No. R76-12, Dept of Civ. Engng, MIT. Cambridge, MA, 115.

Hiew, S. Y., Teoh, K. Bin, Raman, S. N., Kong, D., & Hafezolghorani, M. (2023). Prediction of ultimate conditions and stress–strain behaviour of steel-confined ultra-high-performance concrete using sequential deep feed-forward neural network modelling strategy. Engineering Structures, 277, 115447. https://doi.org/10.1016/J.ENGSTRUCT.2022.115447

Hu, J., Liu, M., & Tan, J. (2022). Damping Modification Factors for Horizontal and Vertical Acceleration Spectra from Offshore Ground Motions in the Japan Sagami Bay Region. Bulletin of the Seismological Society of America, 112(5), 2621–2641. https://doi.org/10.1785/0120210327

Kareem, A. (1988). Aerodynamic response of structures with parametric uncertainties. Structural Safety, 5(3), 205–225. https://doi.org/10.1016/0167-4730(88)90010-0

Kareem, A., & Gurley, K. (1996). Damping in structures: its evaluation and treatment of uncertainty. Journal of Wind Engineering and Industrial Aerodynamics, 59(2–3), 131–157. https://doi.org/10.1016/0167-6105(96)00004-9

Kayhan, A. H., Demir, A., & Palanci, M. (2018). Statistical evaluation of maximum displacement demands of SDOF systems by code-compatible nonlinear time history analysis. Soil Dynamics and Earthquake Engineering, 115, 513–530. https://doi.org/10.1016/J.SOILDYN.2018.09.008

Lin, Y. Y., & Chang, K. C. (2003). Study on Damping Reduction Factor for Buildings under Earthquake Ground Motions. Journal of Structural Engineering, 129(2), 206–214. https://doi.org/10.1061/(ASCE)0733-9445(2003)129:2(206)

Liu, T., Wang, W., Wang, H., & Su, B. (2021). Improved damping reduction factor models for different response spectra. Engineering Structures, 246, 113012. https://doi.org/10.1016/J.ENGSTRUCT.2021.113012

Moustafa, A., & Mahadevan, S. (2011). Reliability analysis of uncertain structures using earthquake response spectra. Earthquakes and Structures, 2(3), 279–295. https://doi.org/10.12989/eas.2011.2.3.279

Pennucci, D., Sullivan, T. J., & Calvi, G. M. (2011). Displacement reduction factors for the design of medium and long period structures. Journal of Earthquake Engineering, 15(SUPPL. 1), 1–29. https://doi.org/10.1080/13632469.2011.562073

Taylor, P., Pennucci, D., Sullivan, T. J., & Calvi, G. M. (n.d.). Displacement Reduction Factors for the Design of Medium and Long Period Structures Displacement Reduction Factors for the Design of Medium and Long Period Structures. December 2014, 37–41. https://doi.org/10.1080/13632469.2011.562073

Zhang, H., & Zhao, Y. G. (2021). Damping Modification Factor of Acceleration Response Spectrum considering Seismological Effects. Journal of Earthquake Engineering, 00(00), 1–24. https://doi.org/10.1080/13632469.2021.1991521

Zhang, H., & Zhao, Y. G. (2022). Effects of magnitude and distance on spectral and pseudospectral acceleration proximities for high damping ratio. Bulletin of Earthquake Engineering, 0123456789. https://doi.org/10.1007/s10518-022-01328-9